INTERNATIONAL JOURNAL OF CIVIL ENGINEERING AND TECHNOLOGY (IJCIET)

IJCIET

©IAEME

FRICTION MECHANISMS OF FRESH CONCRETE UNDER PRESSURE

Y. Vanhove,   C. Djelal

Professor, Dept. of Civil Engineering, LGCgE , University Lille Nord of France

ABSTRACT

Ensuring adequate placement of concrete on site requires special consideration of rheological properties and concrete/wall interface. However, few studies were conducted on phenomena existing at the interface and particularly when the concrete is under pressure. Friction occurs in many applications in civil engineering field as slipforming, concrete pressure on formwork, or on the concrete facing quality. This paper provides experimental results to enable a better understanding of friction mechanisms. Many parameters that influence friction are being studied on different types of concrete. Friction tests on fresh concrete have been carried out using a plane/plane tribometer. Critical pressures and sliding velocities appear depending on the plate roughness and the mix design. Concerning the mix design, grains size and the water reducing agent play an important role on the friction stress. These results can contribute to adapt mix design according to the application and to perform models based on the fresh concrete friction.

Keywords: Friction, Interface, Fresh Concrete**,** Tribometer, Boundary Layer

1. INTRODUCTION

Even though design issues should be the primary consideration among formwork manufacturers, demands imposed by clients and project owners have become increasingly predominant in this field. The recent emphasis on technique and quality in the execution of cast elements stems from the vital economic interest these elements represent. The quality of concrete surfaces may be affected by a colour variation, the heterogeneity or the appearance of bubbling. The parameters able of influencing the appearance of this type of defect include concrete placement in the formwork, characteristics of the formwork wall (surface condition), and the effect of a formwork release agent.

Formwork is designed to resist at the concrete pressure. Previous studies [1, 2] were conducted in order to determine concrete pressure during pouring into a formwork. For self-compacting concretes, the pressure exerted on the formwork P_{trib} vs. formwork height has been estimated by the following expression:

$$P_{trib}(z) = \frac{\rho g(e \times L)}{f(2e+2L)(1-\sin\varphi)\mu}\left[1 - \exp^{-\frac{f(2e+2L)(1-\sin\varphi)\mu}{(e\times L)}z}\right] \qquad (1)$$

This approach makes use of a friction stress that in turn depends on the concrete/wall interface conditions. Even nowadays, this parameter remains difficult to estimate. While the friction of solid materials can be derived with precision, such is not the case for fresh concrete, which does not qualify as a continuous medium, but instead as a dense suspension containing a mix of water, adjuvant and particles with a very wide size distribution, extending from smaller than the microcosmic scale to a full centimetre. Moreover, given the complexity of concrete as a material, the surface condition of the formwork skin evolves as the formwork is reused repetitively. This wear has to be taken into account in developing pressure prediction models.

Other studies have been carried out with the backing of manufacturers of formwork and demoulding oils [3-5] for the purpose of determining the influence of such oils on both the quality of facings and the protection of metal formwork walls against corrosion.

An observation of facing surfaces yields two findings: the facing appearance is of higher quality when using new moulds, and a better facing appearance is generated by applying a conic nozzle set-up on a used mould. On the other hand, it would be preferable to spray and then scrape the oil film for a new mould. Fig. 1 shows the surface appearance for a new and old formworks. The following figures show concrete facings generated by applying vegetable oil on both a new mould (Fig. 2a) and used mould (Fig. 2b).
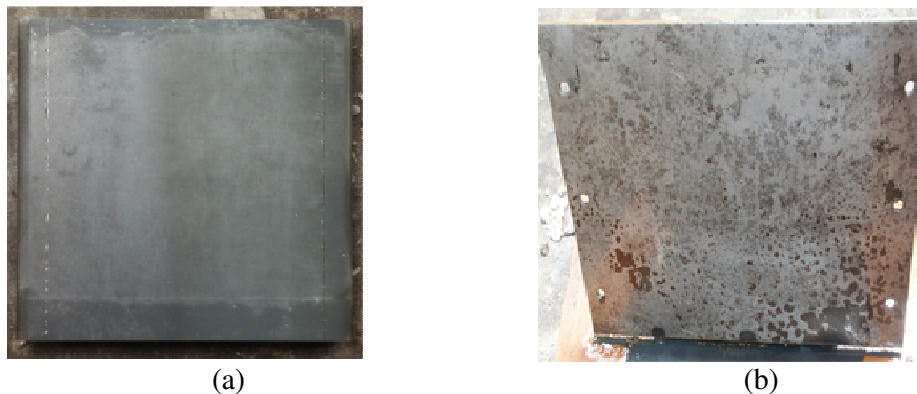

(a)   (b)
Fig. 1 : Formwork surface: (a) new wall; (b) used wall

(a)   (b)
Fig. 2 : Concrete facing: (a) with a new wall; (b) with used wall

The appearance of facings in the latter case is correlated with the wall surface modification, which stems from surface wear as well as corrosion occurring in the presence of water contained in the concrete.

Mechanisms capable of governing wear involve the friction arising when filling the formwork with concrete. Knowledge of a such friction and mechanisms proves to be critical to not only improving mitigation of harmful impacts (facing appearance, wall wear) but also optimising the eventual beneficial aspects (can reduce concrete pressure).

An understanding of behaviour at the concrete/wall interface must be assessed within the scope of a behaviour type generally used in the field of tribology.

Over the past few years, several researchers have focused on friction occurring at the concrete/wall interface. Most authors agree on the fact that the tribological behaviour of fresh concrete at this interface basically depends on: the concrete mix design, wall roughness [6] and the rheological properties of concrete directly in contact with the plate. More specifically, for this latter parameter, various studies have revealed the existence at the concrete/wall interface of a thin layer (also called the boundary layer or third-body inspired by lubrication theory), composed of fines (cement and additions) and water [7]. In the present study, the term fine refers to all grains with a diameter of less than 80 µm. These components are mostly present in the cement and additions. The boundary layer texture corresponds to a paste with a different mix design and rheological properties than the paste inside the concrete volume.

The tribometer employed herein has already been described in detail in the literature [8]. The device makes use of a plane/plane contact by placing a mobile metal plate into contact with a fresh concrete surface.

Friction at the concrete/wall interface depends not only on the properties of contact surfaces and sliding surfaces but also on the behaviour of the separating interface [3]. The respective roles of contact pressure, concreting speed and concrete rheological characteristics will be discussed in this paper.

2. CHARACTERISTICS OF FORMWORK WALLS

The main parameter characterising formwork walls is wall roughness (as manifested by slight surface irregularities). Despite being machined with great care, the surface of a solid always displays some degree of roughness, primarily reflected by the height and local shapes of asperities.

The international roughness parameter is Ra, which measures the mean arithmetic deviation relative to the average line. A second parameter, denoted Rt, has been introduced to determine the distance between the highest and lowest peaks on the profile, as indicated in Fig. 3. This is the parameter we have selected to study the influence of formwork wall roughness. It is important to know the value of parameter Rt for determining whether the constituent concrete grains are in fact capable of lodging inside the slight asperities. Once blocked in the plate roughness, these grains may disrupt order in the material layer near the wall. Such grains are mainly found in cement, sand and addition like limestone filler.
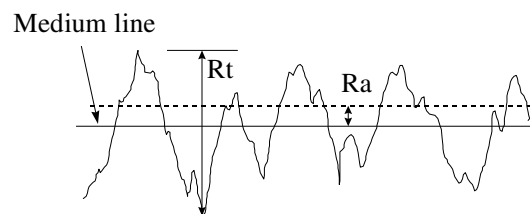

Fig. 3 : Schematic representation of roughness profiles

A series of plates were cut from both new and used formwork walls, built using a C35 steel compliant with the requirements issued in the EN 10277-2 Standard. The used plate was cut from a 7 to 8-year-old form panel that had already been applied 500 to 600 times. Formwork roughness was measured on these plates by means of a portable tactile roughness meter, yielding: Ra = 0.3 µm and Rt = 2.3 µm for the new plate, and Ra = 1.6 µm and Rt = 13.6 µm for the used plate. It should be noted that the machining streaks or grooves are oriented in the direction of plate displacement.

Research [9] conducted on clay paste friction has revealed that roughness exerts a noteworthy influence on friction stress. It has been established that this stress increases in cases where the roughness measurement deviates from the average clay particle size. During repeated passes of clay paste on the wall surface, a surface polishing effect can be observed, as reflected by a drop in the Rt value. In contrast, such is not the case for the used surface in contact with the concrete, which results in a greater distance between the highest and lowest peaks on the profile as well as a widening between any two successive peaks.

3. TESTED CONCRETE SPECIMENS

Three concretes featuring different levels of workability were selected for this study (Table 1). The normal concrete (NC), i.e. containing no admixtures, is primarily used for casting structural element. The concrete with admixtures (FC), and self-compacting concrete (SCC) were mixed as part of a study protocol examining the concrete pressure on formwork, over a wall height of respectively 7 and 12 meters.

Three well-graded sands have been used for the purpose of this study. The first one (Sand 0/3.15) is a sand rolled with a fineness modulus of 2.52, a specific gravity of 2.70, and an absorption value of 1.2 %. Second sand presents a continuous particle size distribution ranging from 0.08 to 4 mm (Sand 0/4) with a fineness modulus of 2.40, a specific gravity of 2.65, and an absorption value of 0.92. The third sand is a combination of two crushed sands in 8:2 proportions, by mass, characterised by a 2.48 fineness modulus, a 2.60 specific gravity, and an absorption value of 2 %. Two types of coarse aggregate (4/10 and 10/20), are retained for the SCC1 with a specific gravity of 2.64 and 2.70, and an absorption coefficient of 0.4 and 0.45%, respectively. Coarse aggregate in the concrete FC have a particle size distribution ranging from 4 to 20 mm (4/20), a specific gravity of 2.67, and an absorption coefficient of 1.8 %.

Constituent material	Units	NC	FC	SCC
Cement C1	Kg/m^3	329		280
Cement C2			350	
Fillers	Kg/m^3			170
Sand 0/3,15	Kg/m^3			735
Sand 0/4 R	Kg/m^3	840	775	
Coarse aggregate 4/10	Kg/m^3	500		260
Coarse aggregate 10/20	Kg/m^3	404		645
Coarse aggregate 4/20	Kg/m^3		965	
HRWR1	L			2.6
HRWR2	L		2,8	
Water	L	201	200	210
Water/Binder*		0.61	0.57	0.46
Coarse aggregate / Sand		1.1	1.25	1.23
Paste volume	%	30.7	31.3	36.4
Specific gravity	Kg/m^3	2274	2293	2302

* Binder: Cement + Fillers

Table 1 : Mix proportions

A high-range water-reducing agent (HRWR1), specially adapted for self-consolidating concrete workability, was used. This HRWR1 is a vinyl copolymer of naphthalene sulphonate with a specific gravity of 1.1 and a solid content of 20.5. A naphthalene-Na superplasticizer (HRWR2) with a specific gravity of 1.2 and a solid content of 40 % is introduced in the FC concrete. Estimates of both the yield stress and plastic viscosity were derived based on a number of predictive equations proposed in the literature [10-12].

For the concrete BN and BF [11-12]:

$$\tau_0 = \frac{\rho}{34,7}(30 - s) + 212 \tag{2}$$

$$\frac{\mu_{visc}}{\rho T'} = Max\left[25; 10.8(s - 17.5)\right] \tag{3}$$

where μ_{visc} is the plastic viscosity of the concrete (expressed in Pa.s), ρ is the concrete density (kg/m^3), T' is the partial slump time when the concrete reach 10 centimetres (second), and s is the final slump (cm).

   − For the SCC [13] :

$$\tau_0 = (808 - S)\frac{\rho g}{11740} \tag{4}$$

$$\mu_{visc} = \frac{\rho g}{10000}(0.026 S - 2.39) \times t_{500} \tag{5}$$

with S is the slump flow (mm), g is the gravitational acceleration, and t_{500} is the time required once the cone has been lifted for the concrete to reach a 500-millimetres disc.

Table 2 lists the average of the range of values obtained. Five test runs were performed for each concrete composition. The average time elapsed by SCC to reach the 500-mm circle was calculated at 5.5 s. The viscosities for the NC and FC specimens could not be determined due to the small value of time T'. Uncertainty on the measurement of this magnitude has caused major viscosity variation, as estimated according to Equation (3).

Type of concrete	Yield stress τ_0 (Pa)	Plastic viscosity μ_{visc} (Pa.s)
BN	1260	—
BF	1070	—
BAP	208	190

Table 2 : Rheological Characteristics of concretes

All mixtures were prepared in 40 L batches in an 60 L capacity pan mixer. The mixing sequence of the concretes was carried out by firstly adding the aggregates and the binder for all mixtures. Once a homogeneous mixture was obtained the following mixing sequence was used depending on the type of concrete.

NC [Aggregates + Binder] —1 minute→ [Water] —2 minutes→ [End of mixing]

FC and SCC [Aggregates + Binder] —1 minute→ [Water +HRWRA2] —2 minutes→ [End of mixing]
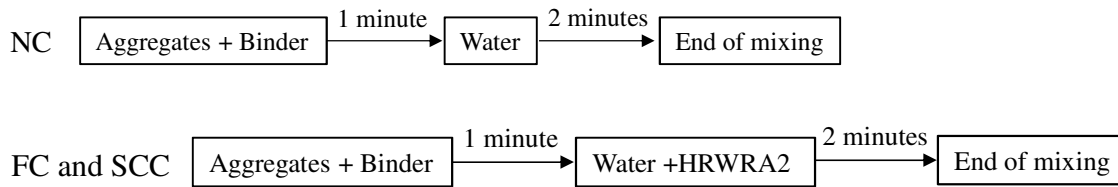
4. THE TRIBOMETER

The principle of this device was inspired by the box shear apparatus used in soil mechanics (Fig. 4). It can reproduce the conditions encountered by manufacturers of concrete walls and precast elements. In particular, it can create sliding contacts between concrete, release agent and formwork [8].
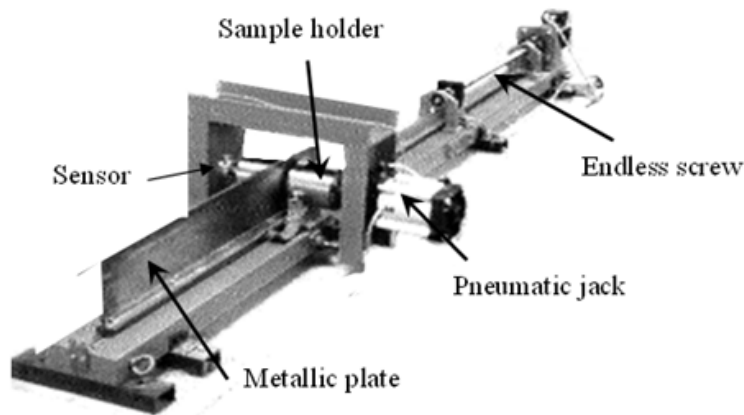

Fig. 4 : Description of The Tribometer

Two 120 mm diameter cylinders, with the concrete inside, were placed either side of a metal plate. The sample-holders were fitted with a gasket system to prevent water egress. The plate was set in motion using a motor coupled to an endless screw. Plate travel was 800 mm. The concrete was pressured against the plate by a jack. The displacement velocity varies from 0 to 300 mm.s^{-1} when the pressure applied to the sample is fixed among a range of 0 to 1700 kPa. A system of joins maintains the material in the sample holding. The inner diameter of the sample-holder and the concrete sample thickness is equal to 120 mm in order to take into consideration the grains size of studied material. The traction force F_{mes} that gives movement to the plate for a fixed sliding velocity is measured by mean of an acquisition device. The force F_{mes} measured results from one part of parasite friction forces F_{par} due to the joins-plate friction and from the resultant of tangential friction forces of the two half sample of the medium studied against the plate (considering the symmetry of the system). The area in contact between the concrete and the plate is calculated from the diameter of the sample-holder. In our case, this area is S_c = 113.1 cm². The frictional, or tangential, stress was calculated by the equation:

$$\tau_f = \frac{F_{mes} - F_{par}}{2 \times S_c} \qquad (6)$$

The rates of concrete injection into formwork lie on the order of 0.5 to 1 m³/h at field sites, which corresponds to concrete rising in the formwork at speeds of between 2 and 20 mm/s. The normal pressure (i.e. 30, 50, 70 and 90 kPa) corresponds to the pressure exerted by concrete on formwork heights of 1.2, 2, 2.8 and 3.6 m, respectively. The pressures evaluated for these tests correspond to the range of pressure values measured at the formwork base. Moreover, the plate displacement speed matches the concrete pouring speed, i.e. 6 m/hr, or 1.67 mm/s.

5. INFLUENCE OF ROUGHNESS AND CONTACT PRESSURE ON THE VARIOUS CONCRETE MIX DESIGNS

Figs. 5a and 5b show the evolution in friction stress vs. contact pressure for the 3 concrete specimens under study. The curve trend is identical for all 3 concretes and the 2 roughness values.
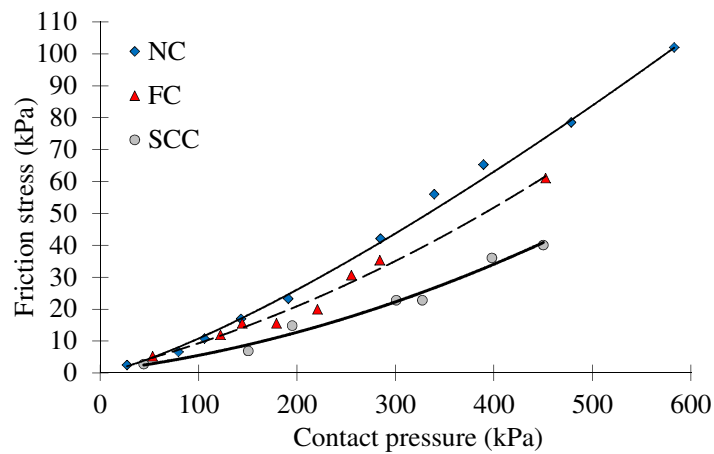
(a)
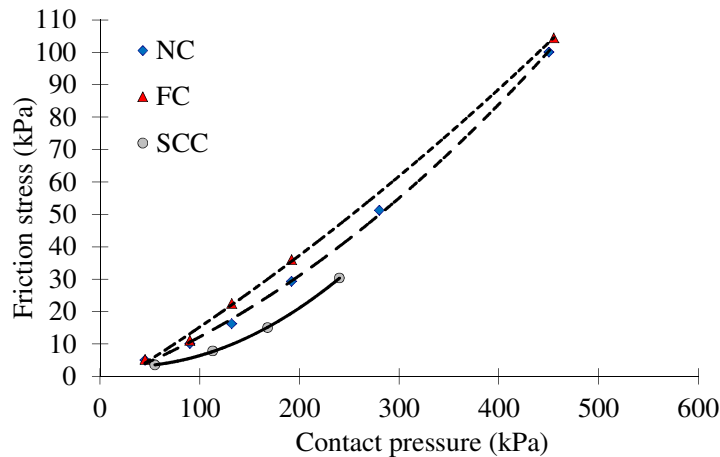
(b)

**Fig. 5 : Evolution of the friction stress according to the contact pressure:
v = 2.5 mm/s; (a) Ra = 0.3 μm, (b) Ra = 1.6 μm**

In spite of its appearance, concrete does not behave as a continuous medium. During concrete placement, a thin layer of paste (thickness: *e*, composed of water and fines particles) occupies the concrete/wall interface zone (i.e. the boundary layer). The various elements will play specific roles during the friction process. For all concretes tested, the normal stress (contact pressure) applied to the material has been transmitted to the granular phase and then to the paste containing binder (itself composed of cement and filler). In the presence of shear, this stress will produce a reorganisation of the various concrete constituents at the concrete/wall interface.

In order to prove the existence of this boundary layer, concrete is introduced into the tribometer sample holders in two successive layers, whereby each layer is perforated by 25 punches, analogously to the Abrams cone, to obtain the appropriate level of concrete compaction and homogeneity. The concrete under pressure has been subjected to a friction test carried out at a rate of 1.6 mm/s; the samples were then preserved in the sample holder under the selected test pressure until their ultimate hardening. Demoulding took place 24 hours after concluding the test, at which point the concrete specimen was cut into 8 slices with thicknesses of 5 ± 2 mm and numbered from N1 (for a surface in contact with the plate) to N8 (a surface 5 mm from the mobile bottom).

Fig. 6 displays the cuts made on the specimens of various concrete compositions, with a paste volume varying from 28% to 34% under a 90-kPa pressure. Identical observations were recorded for pressures of 30, 50 and 70 kPa (see Table 3).
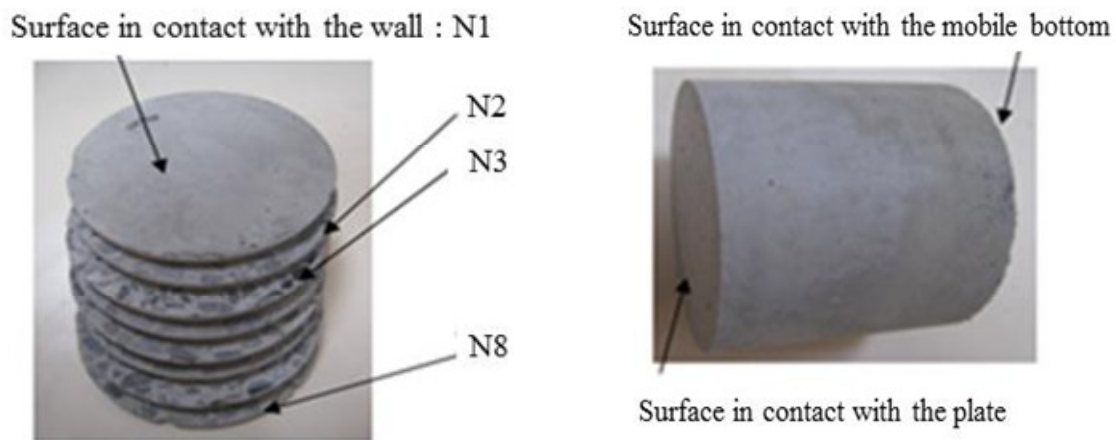

Fig. 6: Cutting the sample into 8 cylindrical slices

The N1 cut is shown on both its faces (front: surface in contact with the plate). The N3 cut provides a representation of the volume measurement of concrete.
The N8 cut corresponds to the last specimen slice. The visible part in Table 3 is positioned 5 mm from the mobile bottom. This N8 cut in its hardened state does not differ in any substantial way from the N1 back surface. The N1 front surface and N8 in contact with the mobile bottom both present a zone with a high concentration of fines.

In the case of concrete C28, several small cavities can be detected before their disappearance, in conjunction with increased paste volume, to yield a more homogeneous surface. Since the C28 specimen contains less paste, it fills the space between the plate and larger-sized elements less readily. These cavities appear regardless of the pressures being exerted on concrete C28.
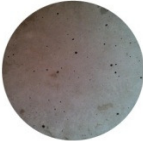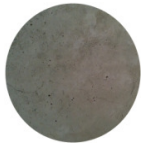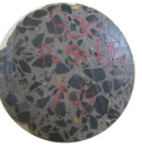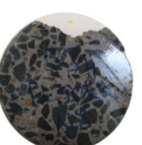
	P = 90 kPa			
	N1 front	**N1 back**	**N3**	**N8**
C28				
C30				
C32				
C34				

Table 3 : Photos of specimen slices for a pressure of 90 kPa [13]

Determining both the composition and properties of this interface layer proves essential to fully understanding the phenomena affecting the concrete/formwork interface.
Ngo [6] and Bouharoun [13] demonstrated that paste volume had very little influence on the composition of the boundary layer present at the concrete/wall interface. The particle size distribution analysis of this layer has indicated that the maximum grain diameter equals 1.25 mm. Grains with diameters above 80 µm originate exclusively from sand. The particle size distribution curves of cement and limestone filler both include grain sizes less than 80 µm.

The increase in paste volume within the concrete will give rise to a thicker boundary layer, regardless of contact pressure. The paste contained in the concrete serves to both lubricate inter-grain contacts and fill spaces that cannot be occupied by elements around 1 millimetre in size (sand, coarse aggregate). Due to the wall effect at the time of application, the concrete will release a specific quantity of paste in the plate direction. The NC specimen displays the smallest paste volume, which might partially explain the higher friction associated with this concrete. Its boundary layer is thinner than that of the other concretes tested.

Excluding paste volume, the evolution presented in Figs. 5a and 5b can also be correlated with the presence of admixture in the concrete samples. The grain-grain and grain-plate contacts are both lubricated to some extent, with the concrete exhibiting less resistance to plate displacement.

For all concretes tested, regardless of the pressure or roughness value, a critical pressure distinguishing two types of concrete behaviour can be observed. This critical pressure may be estimated graphically for each concrete mix composition (Fig. 7).

(a)

(b)

(c)
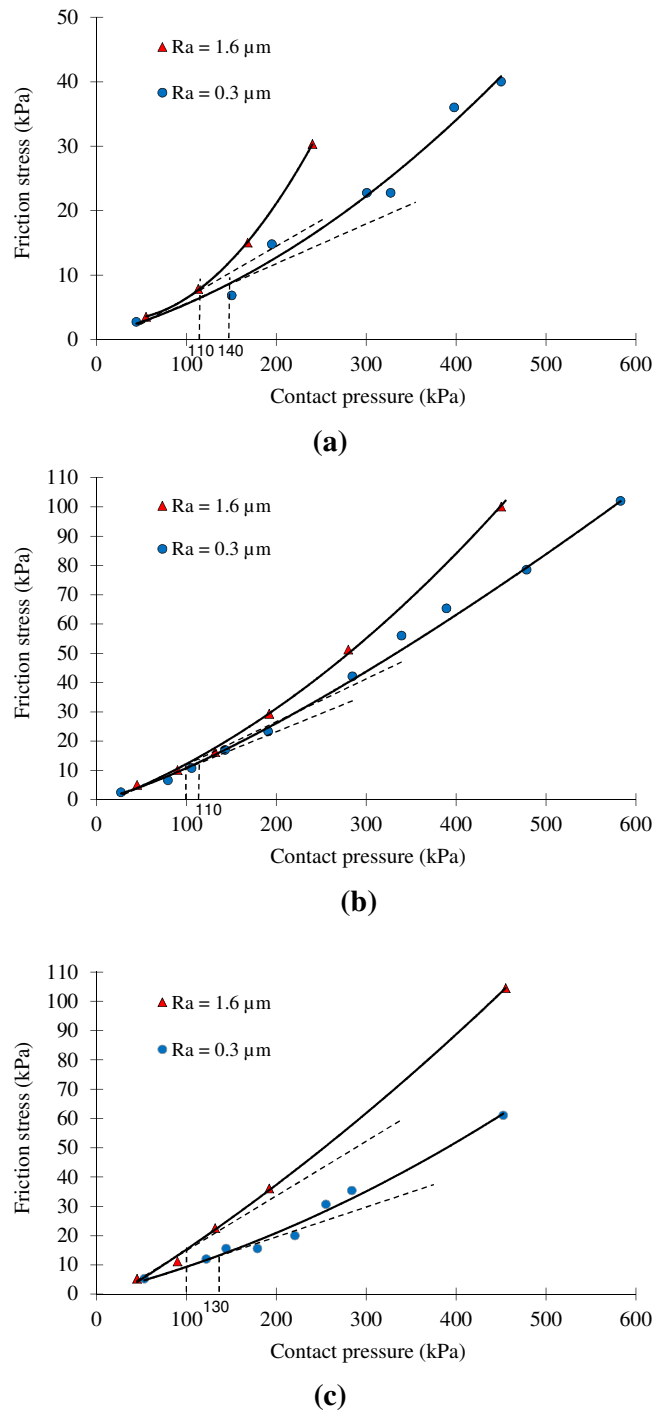
Fig. 7: Variation of the friction stress with the contact pressure: (a) SCC, (b) NC, (c) FC

The critical pressure for the NC specimen has been estimated at 110 kPa for a roughness value of 0.3 µm. For FC, this pressure seems to be higher yet remains below the outcome for the self-compacting concrete specimen (P_{cr} = 140 kPa). The difficulty involved in obtaining an accurate value of critical pressure across all concrete samples is due to the gradual change in boundary layer behaviour. The minimum 5% higher paste volume compared to the other two concretes tested allows

maintaining a sufficient paste quantity prior to the appearance of granular behaviour. Nonetheless, critical pressure will not exceed 150 kPa (Table 4) since this value corresponds to the limit for a concrete material [14].

	NC		FC		SCC	
Ra (µm)	0.3	1.6	0.3	1.6	0.3	1.6
Critical pressure (kPa)	110	100	130	100	140	110

Table 4 : Critical pressures according to the roughness Ra

The relatively smooth plate (roughness: 0.3 µm) does not offer deep enough grooves for the boundary layer to drift; instead, this layer remains trapped at the concrete/plate interface, where it becomes pressurised and absorbs a portion of the normal stress. For concretes designed with a thinner (SCC, FC), shearing inside the boundary layer is facilitated given the deflocculated state of the cement grains, thus resulting in a lower friction stress (Fig. 8a).

As pressure increases ($P > P_{cr}$), a reorganisation quickly takes place at the interface (Fig. 8b), giving rise to contacts between the top of protrusions or irregularities and grains in the granular phase. The force exerted on these tops during plate displacement will cause the grains to rotate, which in turn leads to significant energy dissipation, hence an increase in friction stress and further wear of the metal surface. After a series of tests corresponding to 70 passes of concrete over the plate, the grains were actually responsible for both widening and deepening the irregularities. An Ra value of 2 µm and an average Rt of 26.8 µm were measured. When plate roughness Ra equals 1.6 µm, the friction stress resembles the previous case for pressures below the critical pressure. Roughness Rt equals 13.6 µm, which enables lodging a portion of the boundary element components inside the irregularities. Shear primarily occurs in this layer (Fig. 8a), a finding that also explains why the friction stress value is lower for SCC.
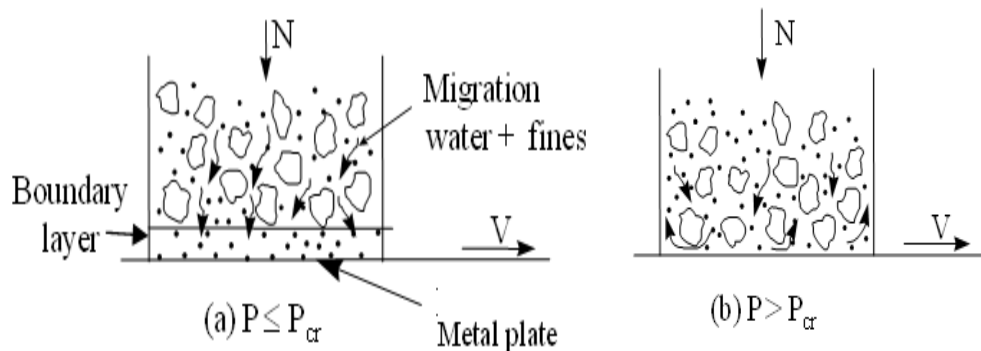

Fig. 8: Schematic representation of a concrete/metal plate interface (Ra = 0.3 µm)

For pressures above the critical level, a portion of the boundary layer will migrate towards less stressed zones (Fig. 8b). The grains stemming from sand or coarse aggregates will then be in direct contact with the tops of irregularities. The force exerted by these tops during plate displacement will wind up causing them to rotate, thus leading to considerable energy dissipation followed by higher stress and metal plate wear. These observations reveal the importance of the size of irregularities compared to grain dimensions. Regardless of the composition tested within the scope of this study, the phenomena occurring at the interface remain identical.

6. INFLUENCE OF SLIDING SPEED

Fig.9 shows the evolution in friction stress vs. speed for all 3 concrete compositions studied using a plate with roughness Ra equal to 0.3 µm.
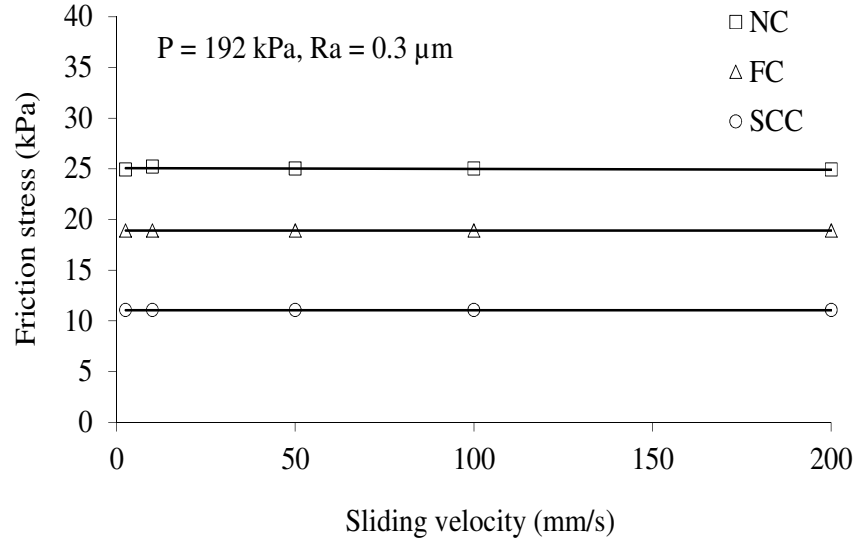

Fig. 9: Variation of the friction stress with the sliding velocity

It would appear that friction stress does not vary with respect to speed according to any set pressure. The average groove depth (Rt = 2.3 µm) does not allow boundary layer fines to locate between pores of the irregularities. The shear gradient induced by plate displacement in the boundary layer thickness remains very small; hence, the evolution in friction stress depends solely on the contact pressure of concrete against the plate, at a roughness Ra equal to 0.3 µm (Fig. 10).
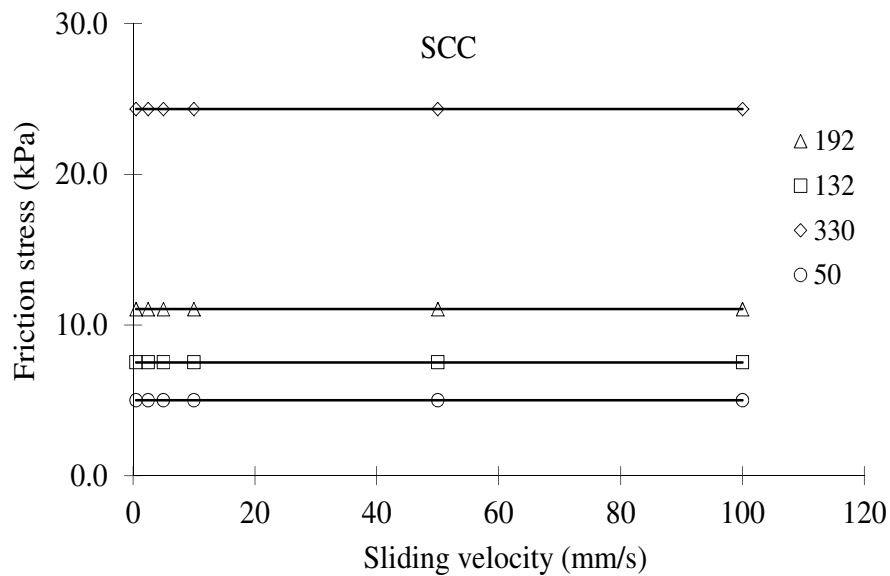

Fig. 10: Variation of the friction stress with the sliding velocity

The curves in Fig. 11 depict friction stress for the 3 test concretes over a range of speeds between 0.5 and 100 mm/s. The contact pressure amounts to 200 kPa for a roughness of 1.6 µm, in surpassing the critical pressure. This higher plate roughness serves to raise the shear gradient within the boundary layer. Friction stress is therefore evolving with respect to plate sliding speed.
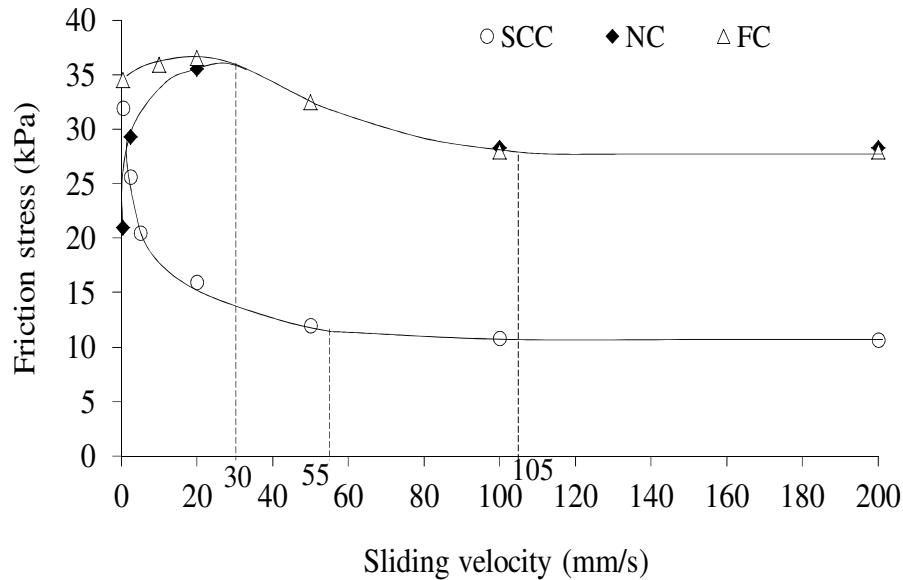

Fig. 11: Variation of the friction stress with the sliding velocity (P =200 kPa; Ra = 1.6 μm)

For this roughness value, the friction stress trend line differs substantially up to a speed of approx. 30 mm/s. Beyond this threshold, a speed decrease is observed to around a threshold starting at 55 mm/s for self-compacting concrete and about 105 mm/s for FC and NC.

At a speed of 1.67 mm/s, the NC specimen displays the lowest friction stress among all tested concretes. This phenomenon is likely correlated with the NC specimen's more limited irregularity filling power (due to its quantity of paste, a non-additive mix) as well as with the number of fines being less than the equivalent number for other compositions. Plate irregularities contain fewer grains, and the concrete winds up being less disturbed within the studied pressure range.

For both NC and FC, an increase in friction stress is recorded between 0 and 30 mm/s. This finding may be explained by the higher shear rate in the boundary layer as plate displacement accelerates. The most marked evolution in NC is due to the somewhat reduced mobility of grains composing the boundary layer. Shear is applied with difficulty. This speed zone up to 30 mm/s highlights the effect of admixture present in the FC concrete or else the speed is exerting less impact on the friction stress increase.

Beyond 30 mm/s, friction stress is seen to be dropping towards a threshold. The sliding speed required to form a shear plane that will only be minimally disrupted by the grains can be estimated at 55 mm/s for SCC and 105 mm/s for NC and FC. Above these respective speeds, the friction stress value is the same for both concretes, which may be due to their closely overlapping yield points.

Fig. 12 shows the evolution in SCC friction stress vs. sliding velocity at various pressures. Let us note that for a pressure level below critical, friction stress does not vary with shear velocity. In this case, shear occurs inside the boundary layer.
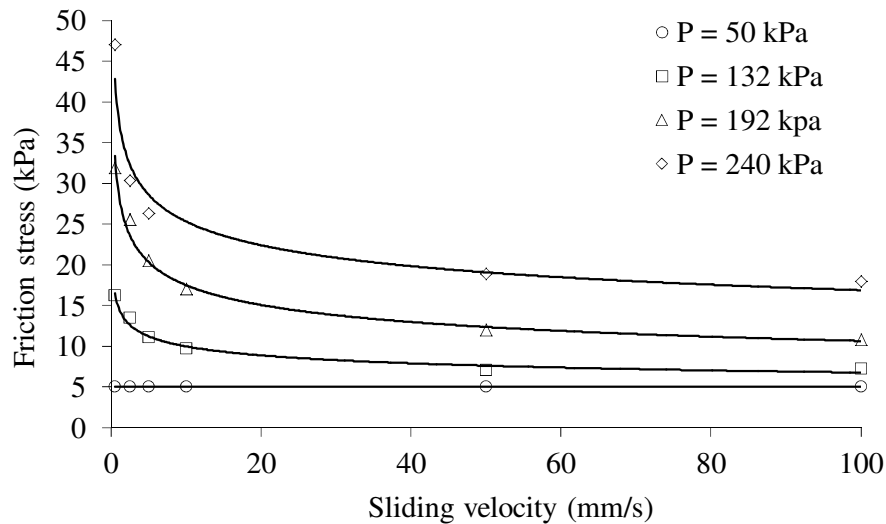
Fig. 12: Variation of the friction stress with the sliding velocity

For pressures above the critical pressure, friction stress depends on velocity; it starts out decreasing and then plateaus at speeds greater than 25 mm/s. For lower velocities, higher stress values are indeed recorded. The shape of these curves is very close to the Stribeck curve, which translates the behaviour of a lubricant in tribology. In our case, the boundary layer is acting as the lubricant.

In Fig. 12, when $0.5 < v < 25$ mm/s, under the effect of pressure, part of the boundary layer will become lodged in plate irregularities and flow into the grooves as a result of plate displacement. Next, the grains trapped inside the pores will cause a grain rotation for the concrete in contact with the wall and adjacent to it, a situation that will lead to a major loss of energy. Such energy dissipation, as reflected by a rise in friction stress, fades as speeds increase ($v > 25$ mm/s), in which case the grains are given less time to move and display their shear resistance. Moreover, shear will occur in the boundary layer, which will lack sufficient time to flow. Friction coefficient values are thus very close to the value identified for a smoother plate. These results have been replicated at other pressures and for the other concretes tested.

7. CONCLUSION

For a velocity of 0.5 mm/s, the NC specimen produces the lowest friction stress values among all concretes tested, a finding likely correlated with this specimen's more limited filling power (resulting from the quantity of paste in the mix) as well as with the fewer number of fines relative to the other mix designs. Plate irregularities contain fewer grains, and the concrete turns out to be less disrupted within the range of test pressures.

It has been shown that for self-compacting concretes, the grains feature extensive mobility and moreover are able to rotate. As the shear rate rises, these grains have less time to move, which causes a drop in friction stress. In the case of the FC specimen, the grains spaced closely together are more heavily constrained in their rotational movement. Shear in the boundary layer does not occur as readily; friction stress increases more abruptly for the NC specimen, given that it has not been designed with an adjuvant (superplasticizer).

As of a certain shear stress value determined by the plate scrolling speed, the grains are no longer able to counter the motion. At this point, a shear plane occurs in the boundary layer, according to the same principle in effect for the self-compacting concrete. Friction stress decreasing towards a

threshold can be observed. The sliding speed necessary to form a shear plane just slightly disturbed by the grains may be estimated at 20 mm/s for the FC specimen and 30 mm/s for NC. Beyond these velocities, the friction stress value is the same for both concrete mixes, perhaps as a result of their similar levels of workability.

REFERENCES

1. Vanhove Y, Djelal C (2004) Prediction laterale pressure by self-compacting concrete on formwork, *Magazine Concrete Research* 56(1):55-62.
2. Hee Kwon S, Tri Phung Q, Yong Park H, Hong Kim J, Shah P. S (2011) Effect of wall friction on variation of formwork pressure over time in self-consolidating concrete, *Cement Concrete Research* 41(1):90-101.
3. Djelal C, Vanhove Y, Kesteloot S, Heloun N (2009) Influence of demoulding oils properties on the facings quality and on the formworks protection against corrosion, *Concrete Plant International* 4:42-51.
4. Baty G, Reynolds R (1997) Release agents – How they work, *Concrete International* 52-54.
5. de Brito J, dos Santos R, Branco F.A (2000) Evaluation of the technical performance of concrete vegetable oil based release agents *Materials and Structures* 33:262-269.
6. Ngo T.T, Kadri E.H, Bennacer R, Cussigh F (2010) Use of tribometer to estimate interface friction and concrete boundary layer composition during the fluid concrete pumping *Construction and Building Materials* 24(7):1253-1261.
7. Djelal C, Vanhove Y, Magnin A (2004) Tribological behaviour of self compacting concrete *Cement and Concrete Research* 34:821-828.
8. Vanhove Y, Djelal C, Magnin A (2004) A device for studying fresh concrete friction, *Cement and Concrete Research* 26(2):35-41.
9. Djelal C (2001) Designing and testing of tribometer for the study of friction of a concentrated clay-water mixture against a metallic surface *Materials and Structures* 34(235):51-58.
10. Ferraris C.F, de Larrard F (1998) Testing and modelling of fresh concrete rheology, NISTIR 6094.
11. Kaplan D (2000) Pompage des bétons, Ph.D., ENPC
12. Sedran T. (1999) Rheologie et rheometrie des bétons – Applications aux bétons autonivelants, Ph.D., ENPC
13. Bouharoun S (2011) Comportement tribologique des huiles de décoffrage à l'interface béton/coffrage – Influence de la formulation du béton, Ph.D., Artois University
14. Baudeau P (1983) Contribution à l'étude du comportement rhéologique du béton contenu dans les parois coffrantes de grandes hauteurs avant la prise du ciment, Ph.D., University of Louis Pasteur.
15. N.Ganesan, Bharati Raj, A.P.Shashikala and Nandini S.Nair, "Effect of Steel Fibres on the Strength and Behaviour of Self Compacting Rubberised Concrete", International Journal of Civil Engineering & Technology (IJCIET), Volume 3, Issue 2, 2012, pp. 94 - 107, ISSN Print: 0976 – 6308, ISSN Online: 0976 – 6316.
16. Abbas S. Al-Ameeri and Rawaa H. Issa, "Effect of Sulfate on the Properties of Self Compacting Concrete Reinforced by Steel Fiber", International Journal of Civil Engineering & Technology (IJCIET), Volume 4, Issue 2, 2013, pp. 270 - 287, ISSN Print: 0976 – 6308, ISSN Online: 0976 – 6316.
17. N. Krishna Murthy, A.V. Narasimha Rao, I .V . Ramana Reddy, M. Vijaya Sekhar Reddy and P. Ramesh, "Properties of Materials used in Self Compacting Concrete (SCC)", International Journal of Civil Engineering & Technology (IJCIET), Volume 3, Issue 2, 2012, pp. 353 - 368, ISSN Print: 0976 – 6308, ISSN Online: 0976 – 6316.